Synchronization of Delayed Fuzzy Neural Networks with Probabilistic Communication Delay and Its Application to Image Encryption

Shen Yan, Zhou Gu, *Member, IEEE*, Ju H. Park, *Senior Member, IEEE*, and Xiangpeng Xie, *Member, IEEE*

***Abstract*—In this article, we study the design of fuzzy synchronization controller of Takagi–Sugeno (T–S) fuzzy neural networks with distributed time-varying delay and probabilistic network communication delay. Compared with the existing model of neural networks with distributed time-varying delay without kernel, a more general model containing a distributed delay kernel is considered. By utilizing the probability distribution of random communication delays, a distributed but deterministic delay model is established. In this model, the delay probability density function is treated as the distributed delay kernel. By developing a new Lyapunov–Krasovskii functional related to the distributed delay kernels and using an integral inequality, new sufficient conditions for the existence of a synchronization controller are presented. Finally, a numerical simulation and an application of encrypting the image are carried out to illustrate the effectiveness of the developed strategy.**

***Index Terms*—Distributed delay, neural networks (NNs), probabilistic communication delay, synchronization, Takagi–Sugeno (T–S) fuzzy system.**

I. Introduction

THE Takagi–Sugeno (T–S) fuzzy model is regarded not only as a powerful but also as a simple means to approximate complex nonlinearities, which makes it effective for the analysis and synthesis of practical nonlinear systems [1]–[5]. Some meaningful analysis and design results have been proposed for addressing the filtering problem [6], [7] and stabilization problem [8], [9] of T–S fuzzy systems. On the flip side, neural networks (NNs) have gained much attention from scholars owing to the fact that they have been widely applied in secure communication, pattern recognition, machine learning, and so on [10]–[12]. To implement these applications, one often has to deal with the synchronization problem of NNs, on which a relevant amount of research has been carried out [13]–[15]. In terms of the properties of NNs and T–S fuzzy model, T–S fuzzy NNs are viewed as an effective and important model to describe complex nonlinear systems. Over the past years, the synchronization of T–S fuzzy NNs has been extensively studied in [16]–[19] and the reference therein.

As a common phenomenon in NNs, time delay usually leads to oscillation of the system, which could degrade the system performance and even destroy the system stability [20]. Various results have been obtained to study the stability and stabilization of systems with discrete time delays and distributed delays in [21]–[23] and references therein. To be specific, Song et al. [21] investigated the stability analysis problem of NNs subject to discrete and distributed delays. For a linear time-delay system with distributed delay kernel, Seuret et al. [22] proposed a method based on the Legendre polynomials to approximate the kernel. Different from the distributed constant delay handled in [21] and [22], the stability issues of NNs with distributed time-varying delays are studied in [23], where the distributed delay kernel is not considered. Due to the fact that the polynomials will become nonlinear with regard to distributed time-varying delay, the approximation method in [22] may be difficultly applied to handle NNs with distributed time-varying delays.

On the other hand, networked control systems (NCSs) have received increasing interests due to the benefits, such as low cost and easy maintenance [24]–[26]. As the system loop is closed by a shared network, the time delay induced by data transmission over a wired/wireless network becomes an important issue in the study of NCSs. It is well known that utilizing more information of the delay leads to less conservative result. A proper selection of the delay information should be based on practical considerations. In many existing works, such as [27]–[29], an interval time-varying delay is considered where only the bounded information of delay are involved in stability analysis. In fact, under certain communication protocols, such as the Internet protocol and the IEEE 802.11, transmission delay

Manuscript received 16 May 2022; accepted 20 July 2022. Date of publication 25 July 2022; date of current version 1 March 2023. This work was supported in part by the National Natural Science Foundation of China under Grant 62103193 and Grant 62022044, in part by the Natural Science Foundation of Jiangsu Province of China under Grant BK20200769, in part by the Natural Science Foundation of Jiangsu Provincial Universities under Grant 20KJB510045, and in part by the China Postdoctoral Science Foundation under Grant 2021TQ0155 and Grant 2022M711646. The work of Ju H. Park was supported by the National Research Foundation of Korea (NRF), Korea government (Ministry of Science and ICT), under Grant 2019R1A5A8080290. *(Corresponding authors: Zhou Gu; Ju H. Park.)*

Shen Yan and Zhou Gu are with the College of Mechanical and Electronic Engineering, Nanjing Forestry University, Nanjing 210037, China (e-mail: yanshenzdh@gmail.com; gzh1808@163.com).

Ju H. Park is with the Department of Electrical Engineering, Yeungnam University, Kyongsan 38541, South Korea (e-mail: jessie@ynu.ac.kr).

Xiangpeng Xie is with the Institute of Advanced Technology, Nanjing University of Posts and Telecommunications, Nanjing 210023, China (e-mail: xiexiangpeng1953@163.com).

Color versions of one or more figures in this article are available at https://doi.org/10.1109/TFUZZ.2022.3193757.

Digital Object Identifier 10.1109/TFUZZ.2022.3193757

can be characterized by its probability density function [30], which can be obtained via some statistical approach. In light of this idea, a delay-distribution method is used to study the event-triggered guaranteed cost control issue for Markov jump discrete-time NNs [31] and the synchronization problem of stochastic memristor-based NNs [32], where the time delay is categorized as short and long delays through the introduction of a Bernoulli variable. Yet, utilizing a random variable to describe the delay distribution still corresponds to the cumulative probability, not the specific probability density. To the best of our knowledge, few effort has been devoted to addressing the synchronization issue of NNs subject to distributed time-varying delay with its kernel and random communication delay with its probability density, which motivates the present research.

In terms of the abovementioned observations, this article investigates the synchronization of T–S fuzzy NNs, where the time-varying distributed delay and random network communication delay are considered. Its application to image encryption is developed and the security of the presented algorithm is studied. As the introduction of delay probability density, there exist two challenging problems given as follows to be solved. The first challenge is how to model the random delay by utilizing the probability distribution information. The second one is how to obtain less conservative results for the new delay model without introducing any approximation error, which is inevitable by using the existing approach dependent on Legendre polynomials. To conquer the abovementioned difficulties, the main contributions are listed in the following.

1) A distributed delay $\int_{-\tau_M}^{0} w(s)x(t+s)ds$ with kernel $w(s)$ is employed to represent the probabilistic network delay, where $w(s)$ means the probability density function of delay. Then, the T–S fuzzy NNs with time-varying distributed delay and random communication delay is established in a united distributed delay system with kernels.
2) A novel Lyapunov–Krasovskii functional (LKF) dependent on the distributed kernels is chosen and some integral inequalities are used to deal with the distributed delay terms. Our method can exclude the nonlinear approximation terms related to the distributed time-varying delay introduced by using the existing method based on Legendre polynomials [22]. Then, new sufficient linear matrix inequality conditions that guarantee the asymptotic synchronization of the NNs are developed.

The rest of this article is organized as follows. The theoretical background of modeling the closed-loop T–S fuzzy NNs with probabilistic delay is given in Section II. Then, the control design conditions are derived in Section III. Some simulation results are executed in Section IV. In Section V, the studied synchronization issue is applied to image encryption. Finally, Section VI concludes this article and gives some future investigations.

Notations: In this article, $\mathbf{He}(A)$ is equivalent to $A^T + A$. $\mathbf{Sy}(A, B)$ represents $A^T BA$. $\otimes$ is Kronecker product.

II. Theoretical Background

The T–S fuzzy NN described by IF–THEN rules is considered as follows.

Plant rule i: IF $\phi_1(t)$ is M_1^i, $\phi_2(t)$ is M_2^i, …, AND $\phi_{\mathscr{q}}(t)$ is $M_{\mathscr{q}}^i$, THEN

$$\dot{\delta}(t) = A_i\delta(t) + C_i\eta(\delta(t-r_1)) + N_i\int_{-r(t)}^{0} g(s)\eta(\delta(t+s))ds \tag{1}$$

for $i \in \mathscr{P} \triangleq \{1, 2, \ldots, \mathscr{p}\}$, where $\phi_{\mathscr{ó}}$ and $M_{\mathscr{ó}}^i(\mathscr{ó} = 1, \ldots, \mathscr{p})$ are the $\mathscr{ó}$th premise variable and fuzzy set, respectively. $\delta(t) \in \mathbb{R}^n$ is the state of system, $0 < r_1 \le r(t) \le r_2$, the matrices A_i, N_i, and C_i are system matrices, and $\mathscr{p}$ is the number of IF–THEN rules.

Define $\phi(t) = [\phi_1(t), \ldots, \phi_{\mathscr{q}}(t)]$ and $\vartheta_i(\phi(t)) = \prod_{j=1}^{\mathscr{q}} M_j^i(\phi_j(t))$, where $M_j^i(\phi_j(t))$ is the grade of membership of $\phi_j(t)$ in fuzzy set M_j^i, and the membership function $\theta_i(\phi(t))$ is obtained as

$$\theta_i(\phi(t)) = \frac{\vartheta_i(\phi(t))}{\sum_{i=1}^{\mathscr{q}} \vartheta_i(\phi(t))} \tag{2}$$

where $0 \le \theta_i(\phi(t)) \le 1$ and $\sum_{i=1}^{p} \mu_i(\theta(t)) = 1$. Then, the fuzzy system (1) can be written as

$$\dot{\delta}(t) = \sum_{i=1}^{\mathscr{p}} \theta_i(t) \Big[A_i\delta(t) + C_i\eta(\delta(t-r_1)) + N_i\int_{-r(t)}^{0} g(s)\eta(\delta(t+s))ds \Big]. \tag{3}$$

By taking system (3) as the primary system, the secondary system is introduced as

$$\dot{\sigma}(t) = \sum_{i=1}^{\mathscr{p}} \theta_i(t) \Big[A_i\sigma(t) + C_i\eta(\sigma(t-r_1)) + N_i\int_{-r(t)}^{0} g(s)\eta(\sigma(t+s))ds + u(t) \Big] \tag{4}$$

where $u(t) \in \mathbb{R}^{\mathscr{m}}$ is the control input.

Defining the error term $x(t) = \sigma(t) - \delta(t)$ and combining (3) and (4), one can obtain the synchronization error system as

$$\dot{x}(t) = \sum_{i=1}^{\mathscr{p}} \theta_i(t) \Big[A_ix(t) + C_i\psi(x(t-r_1)) + N_i\int_{-r(t)}^{0} g(s)\psi(x(t+s))ds + u(t) \Big] \tag{5}$$

where $\psi(x(t)) = \eta(\sigma(t)) - \eta(\delta(t))$.

The neuron $\psi(x)$ satisfies

$$(\psi(x) - \Psi_1 x)^T(\psi(x) - \Psi_2 x) \le 0 \tag{6}$$

where Ψ_1 and Ψ_2 are constant matrices meeting $\Psi_2 - \Psi_1 \ge 0$.

It is assumed that for the kernel $g(s)$ of $\int_{-r(t)}^{0} g(s)\psi(x(t+s))ds$, there exists a vector $\boldsymbol{g}(s) = [g_0(s) \ \ldots \ g_i(s) \ \cdots \ g_\varrho(s)]^T$, $g_0(s) \triangleq g(s)$, $i = 0, 1, \ldots, \varrho$, with $\varrho \in \mathbb{N}$ and $s \in [s_1, s_2]$ satisfying the property

$$\frac{d\boldsymbol{g}(s)}{ds} = \mathcal{G}\boldsymbol{g}(s) \tag{7}$$

where $g_i(s)$ are linear independent, $\mathcal{G} \in \mathbb{R}^{\varrho\times\varrho}$, and $\int_{s_1}^{s_2} \boldsymbol{g}(s)\boldsymbol{g}^T(s)ds > 0$.

The control signal is transmitted over the communication network, where the random communication delays are considered. The control law of the jth rule is described as follows.

Control rule j: IF $\phi_1(t)$ is M_1^i, $\phi_2(t)$ is M_2^i, ..., AND $\phi_\varrho(t)$ is M_ϱ^i, THEN

$$u(t) = K_j x(t-\tau(t)) \tag{8}$$

in which K_j is the controller gain designed later and $\tau(t) \in [0, \tau_M]$ is the stochastic transmission delay. Following the similar way to obtain fuzzy system (3), the whole fuzzy controller is derived as

$$u(t) = \sum_{j=1}^{p} \theta_j(t-\tau(t))K_j x(t-\tau(t)). \tag{9}$$

It is noted that the random communication delay $\tau(t)$ usually meets some probability distributions. To make the most of the probability information of $\tau(t)$, a function $w(\cdot)$ is considered to describe its probability density. By approximating a random delay by a deterministic, distributed delay model, a synchronization controller is written as

$$u(t) = \sum_{j=1}^{p} \theta_j^\tau K_j \int_{-\tau_M}^{0} w(s)x(t+s)ds \tag{10}$$

where the probability density $w(s)$, similar to $g(s)$, is assumed to satisfy (7) with $g(s)$ replaced by $w(s)$. In the following derivation, $\theta_i(t)$ and θ_j^τ are abbreviated as θ_i and $\theta_j(t-\tau(t))$, respectively.

With the combination of (5) and (10), we have the closed-loop system as follows:

$$\dot{x}(t) = \sum_{i=1}^{p}\sum_{j=1}^{p} \theta_i\theta_j^\tau \Bigg[A_i x(t) + C_i\psi(x(t-r_1)) + N_i\int_{-r(t)}^{0} g(s)\psi(x(t+s))ds + K_j\int_{-\tau_M}^{0} w(s)x(t+s)ds\Bigg]. \tag{11}$$

Remark 1: In this article, a new model of delay fuzzy NNs with probabilistic network delay is formed as a distributed delay system. Compared with the traditional interval time-varying delay model only using the upper and lower delay bounds, the probability density is considered in our delay model. Therefore, the proposed distributed delay modeling strategy could derive less conservative results.

For simplicity of derivation, we define

$$\mathbb{E}_a \triangleq \begin{bmatrix} 0_{n,(a-1)n} & I_n & 0_{n,(10+3\varrho_1+\varrho_2-a)n}\end{bmatrix}$$

$$\int_{-r_1}^{0} G(s)\psi(x(t+s))ds = \mathbb{G}_1(t)$$

$$\int_{-r_2}^{-r_1} G(s)\psi(x(t+s))ds = \mathbb{G}_2(t)$$

$$\int_{-r(t)}^{-r_1} G(s)\psi(x(t+s))ds = \mathbb{G}_3(t)$$

$$\int_{-r_2}^{-r(t)} G(s)\psi(x(t+s))ds = \mathbb{G}_4(t)$$

$$\int_{-\tau_M}^{0} W(s)x(t+s)ds = \mathbb{W}(t)$$

$$G(s) \triangleq \boldsymbol{g}(s)\otimes I_n, g_0(s) = g(s)$$

$$\boldsymbol{g}(s) = [g_0(s), g_1(s), \ldots, g_{\varrho_1}(s)]^\top$$

$$W(s) \triangleq \boldsymbol{w}(s)\otimes I_n, w_0(s) = w(s)$$

$$\boldsymbol{w}(s) = [w_0(s), w_1(s), \ldots, w_{\varrho_2}(s)]^\top.$$

Then, one gets

$$\int_{-r(t)}^{0} g(s)\psi(x(t+s))ds = \mathcal{I}_1\left(\mathbb{G}_1(t) + \mathbb{G}_3(t)\right) \tag{12}$$

$$\int_{-\tau_M}^{0} w(s)x(t+s)ds = \mathcal{I}_2\mathbb{W}_x(t) \tag{13}$$

where $\mathcal{I}_1 = [\, I_n \; 0_{n,\varrho_1 n}\,]$ and $\mathcal{I}_2 = [\, I_n \; 0_{n,\varrho_2 n}\,]$.

By replacing the integral terms in (11) with (12) and (13), it gives the following synchronization error system:

$$\dot{x}(t) = \sum_{i=1}^{p}\sum_{j=1}^{p} \theta_i\theta_j^\tau \left[A_i x(t) + C_i\psi(x(t-r_1)) + N_i\mathcal{I}_1\left(\mathbb{G}_1(t) + \mathbb{G}_3(t)\right) + K_j\mathcal{I}_2\mathbb{W}_x(t)\right]. \tag{14}$$

This article aims to obtain a controller (10) such that the closed-loop synchronization error system (14) is asymptotically stable.

In order to achieve the results, two useful lemmas are given as follows.

Lemma 1 (See [35]): For $y(s) \in \mathbb{R}^n$, $s \in [a, b]$, a matrix $X \in \mathbb{R}^{n\times n} > 0$, we have

$$\int_b^a \mathbf{Sy}(X, y(s))ds \geq \mathbf{Sy}\left(\mho\otimes X, \int_b^a G(s)y(s)ds\right) \tag{15}$$

for $\mho^{-1} = \int_b^a \boldsymbol{g}(s)\boldsymbol{g}^\top(s)ds > 0$.

Lemma 2 (See [33]): For $y(s) \in \mathbb{R}^n$, $s \in [\underline{r}, \bar{r}]$, a matrix $X \in \mathbb{R}^{n\times n} > 0$, one can obtain

$$\int_{\underline{r}}^{\bar{r}} \mathbf{Sy}(X, y(s))ds \geq \mathbf{Sy}\left(\mathcal{X}\otimes\Omega, \begin{bmatrix}\mathbb{C}_{n,\varrho+1}0_{(\varrho+1)n} \\ 0_{(\varrho+1)n}\mathbb{C}_{n,\varrho+1}\end{bmatrix}\Pi\right) \tag{16}$$

for any $Y \in \mathbb{R}^{n\times n}$ satisfying $\mathcal{X} > 0$, $r(t) \in [\underline{r}, \bar{r}]$ with

$$\mathcal{X} = \begin{bmatrix} X & T \\ T^\top & X\end{bmatrix}, \Pi = \begin{bmatrix}\int_{r(t)}^{\bar{r}} G(s)y(s)ds \\ \int_{\underline{r}}^{r(t)} G(s)y(s)ds\end{bmatrix},$$

and $\Omega^{-1} = \int_{\underline{r}}^{\bar{r}} \boldsymbol{g}(s)\boldsymbol{g}^\top(s)ds > 0$.

Remark 2: $\mathbb{C}_{n,\varrho_1+1} \in \mathbb{R}^{n(r+1)\times n(\varrho_1+1)}$ is used to represent the communication matrix for Kronecker products. Its property can be referred to [33, Lem. 2]. In addition, the MATLAB function $\mathbf{vecperm}(n, (\varrho_1+1))$, proposed by Higham [34], is an effective toolbox to calculate $\mathbb{C}_{n,(\varrho_1+1)}$.

III. Control Design

Before deriving the main results, we construct an LKF as

$$V(t) = V_1(t) + V_2(t) + V_3(t) + V_4(t) \tag{17}$$

where

$$V_1(t) = \mathbf{Sy}(P, \varkappa(t)), \varkappa(t) = \left[x^\top(t)\mathbb{G}_1^\top(t)\mathbb{G}_2^\top(t)\mathbb{W}^\top(t)\right]^\top$$

$$V_2(t) = \int_{-r_1}^{0} \mathbf{Sy}\left(S_1 + (s+r_1)R_1, \psi(x(t+s))\,ds\right.$$

$$V_3(t) = \int_{-r_2}^{-r_1} \mathbf{Sy}\left(S_2 + (s+r_2)R_2, \psi(x(t+s))\,ds\right.$$

$$V_4(t) = \int_{-\tau_M}^{0} \mathbf{Sy}\left(S_3 + (s+\tau_M)R_3, x(t+s)\right)ds.$$

The asymptotic stability criteria of system (14) with probabilistic network delay are achieved in Theorem 1.

Theorem 1: For given scalars τ_M, r_1, r_2 μ, ν, ϑ_1, and ϑ_2 and controller gain K_i, the system (14) is asymptotically stable, if there exist symmetric matrices P, $S_1 > 0$, $R_1 > 0$, $S_2 > 0$, $R_2 > 0$, $S_3 > 0$, and $R_3 > 0$, and matrices T_1, T_2, and Y such that

$$\mathcal{P} > 0 \tag{18}$$

$$\Pi_{ij} + \Theta_{ij} < 0 \tag{19}$$

$$\digamma < 0 \tag{20}$$

$$\beth_{1i} - \frac{(\digamma_{i,l} + \digamma_{l,i})}{2} > 0, i, l = 1, \ldots, \rho \tag{21}$$

$$\beth_{2j} - \frac{(\digamma_{l+\rho,j+\rho} + \digamma_{j+\rho,l+\rho})}{2} > 0, j, l = 1, \ldots, \rho \tag{22}$$

where

$$\rho = P + diag\left\{0, \mathcal{S}_1, \mathbb{S}_2, \mathcal{S}_3\right\}$$

$$\mathbb{S}_2 = \mathbf{Sy}\left(\mathcal{S}_2, \mathbb{C}\right), \mathbb{C} = \begin{bmatrix} \mathbb{C}_{n,\varrho_1+1} 0_{n(\varrho_1+1)} \\ 0_{n(\varrho_1+1)} \mathbb{C}_{n,\varrho_1+1} \end{bmatrix}$$

$$\mathcal{S}_1 = \mho_1 \otimes S_1, \mathcal{S}_2 = \begin{bmatrix} S_2 & T_1 \\ * & S_2 \end{bmatrix} \otimes \Omega_2, \mathcal{S}_3 = \mho_3 \otimes S_3$$

$$\mathcal{R}_1 = \mho_1 \otimes R_1, \mathcal{R}_2 = \begin{bmatrix} R_2 & T_2 \\ * & R_2 \end{bmatrix} \otimes \Omega_2, \mathcal{R}_3 = \mho_3 \otimes R_3$$

$$\mho_1^{-1} = \int_{-r_1}^{0} \boldsymbol{g}(s)\boldsymbol{g}^\top(s)ds, \Omega_2^{-1} = \int_{-r_2}^{-r_1} \boldsymbol{g}(s)\boldsymbol{g}^\top(s)ds$$

$$\mho_3^{-1} = \int_{-\tau_M}^{0} \boldsymbol{w}(s)\boldsymbol{w}^\top(s)ds, \mathscr{Y} = \left(Y\mathbb{E}_1 + \mu Y\mathbb{E}_2\right)^\top$$

$$\Pi_{ij} = \Gamma_{ij} + \mathbf{He}(\mathscr{Y}\mathscr{G}_{ij}) - \nu\mathbf{Sy}\left(\Phi, \mathcal{E}_1\right)$$

$$\Phi = \begin{bmatrix} \Phi_1 & \Phi_2 \\ * & I \end{bmatrix}, \Phi_1 = \frac{\mathbf{He}(\Psi_1^\top \Psi_2)}{2}, \Phi_2 = \frac{\Psi_1^\top + \Psi_2^\top}{2}$$

$$\mathscr{G}_{ij} = -\mathbb{E}_1 + A_i\mathbb{E}_2 + C_i\mathbb{E}_5 + N_i\mathbb{E}_7 + N_i\mathbb{E}_{8+\varrho_1} + K_j\mathbb{E}_{10+3\varrho_1}$$

$$\Gamma_{ij} = \mathbf{He}(\mathbb{M}^\top P\mathbb{H}) + \Xi, r_3 = r_2 - r_1$$

$$\Xi = diag\{0, \Xi_2, \Xi_3, \Xi_4, \Xi_5, \Xi_6, \Xi_7, \Xi_8, \Xi_9, \Xi_{10}\}$$

$$\Xi_2 = S_3 + \tau_M R_3, \Xi_3 = -S_3, \Xi_4 = S_1 + r_1 R_1$$

$$\Xi_5 = S_2 + r_3 R_2 - S_1, \Xi_6 = -S_2, \Xi_7 = -\mathcal{R}_1$$

$$diag\{\Xi_8, \Xi_9\} = -\mathbf{Sy}(\mathcal{R}_2, \mathbb{C}), \Xi_{10} = -\mathcal{R}_3$$

$$\mathbb{M} = \begin{bmatrix} \mathbb{E}_2 \\ \hat{\mathbb{E}}_{r_1} \\ \hat{\mathbb{E}}_{r_2} \\ \hat{\mathbb{E}}_h \end{bmatrix}, \mathbb{H} = \begin{bmatrix} \mathbb{E}_1 \\ G(0)\mathbb{E}_4 - G(-r_1)\mathbb{E}_5 - \widehat{\mathcal{G}}\hat{\mathbb{E}}_{r_1} \\ G(-r_1)\mathbb{E}_5 - G(-r_2)\mathbb{E}_6 - \widehat{\mathcal{G}}\hat{\mathbb{E}}_{r_2} \\ W(0)\mathbb{E}_2 - W(-\tau_M)\mathbb{E}_3 - \widehat{\mathcal{W}}\hat{\mathbb{E}}_{\tau_M} \end{bmatrix}$$

$$\hat{\mathbb{E}}_{r_1} = \begin{bmatrix} \mathbb{E}_7 \\ \vdots \\ \mathbb{E}_{7+\varrho_1} \end{bmatrix}, \hat{\mathbb{E}}_{r_2} = \begin{bmatrix} \mathbb{E}_{8+\varrho_1} + \mathbb{E}_{9+2\varrho_1} \\ \vdots \\ \mathbb{E}_{8+2\varrho_1} + \mathbb{E}_{9+3\varrho_1} \end{bmatrix}, \mathcal{E}_1 = \begin{bmatrix} \mathbb{E}_2 \\ \mathbb{E}_4 \end{bmatrix}$$

$$\digamma = \begin{bmatrix} \digamma_{1,1} & \digamma_{1,2} & \cdots & \digamma_{1,2\rho} \\ \digamma_{2,1} & \digamma_{2,2} & \cdots & \digamma_{2,2\rho} \\ \vdots & \vdots & \vdots & \vdots \\ \digamma_{2\rho,1} & \digamma_{2\rho,2} & \cdots & \digamma_{2\rho,2\rho} \end{bmatrix}, \hat{\mathbb{E}}_{\tau_M} = \begin{bmatrix} \mathbb{E}_{10+3\varrho_1} \\ \vdots \\ \mathbb{E}_{10+3\varrho_1+\varrho_2} \end{bmatrix},$$

$$\Theta_{ij} = -\left(\digamma_{i,j+\rho} + \digamma_{j+\rho,i}\right) - \frac{(\digamma_{i,j} + \digamma_{j,i})}{2} - \frac{(\digamma_{i+\rho,j+\rho} + \digamma_{j+\rho,i+\rho})}{2} + \sum_{l=1}^{\rho} \vartheta_l \left(\beth_{1i} + \beth_{2j} - \frac{(\digamma_{i,l} + \digamma_{l,i})}{2} - \frac{(\digamma_{l+\rho,j+\rho} + \digamma_{j+\rho,l+\rho})}{2}\right).$$

Proof: See Appendix A. ■

Remark 3: According to (18), the positivity of the chosen LKF (17) is relaxed without demanding $P_\varrho > 0$. With this treatment, the obtained results are less conservative compared with some existing outcomes requiring all Lyapunov variables to be larger than zero.

Remark 4: In [22], Legendre polynomials are applied to approximate the kernel $w(s)$, which results in approximation error. Different from the method in [22], we use the integral inequality in [35] to handle it. Then, the approximation error is removed directly and less conservative results are obtained.

Then, sufficient criteria for solving the synchronization controller are deduced as follows.

Theorem 2: For given parameters τ_M, r_1, r_2 μ, ν, ϑ_1, and ϑ_2, the system (14) is asymptotically stable, if there exist symmetric matrices P, $S_1 > 0$, $R_1 > 0$, $S_2 > 0$, $R_2 > 0$, $S_3 > 0$, and $R_3 > 0$ and matrices T_i $(i = 1, 2)$, U_i, and Y such that (18), (20), (21), and

$$\tilde{\Pi}_{ij} + \tilde{\Theta}_{ij} < 0 \tag{23}$$

where

$$\tilde{\Pi}_{ij} = \Gamma_{ij} + \mathbf{He}(\tilde{\mathscr{Y}}\tilde{\mathscr{G}}_{ij}) - \nu\mathbf{Sy}(\Phi, \mathcal{E}_1), \tilde{\mathscr{Y}}_i = \left(\mathbb{E}_1 + \mu\mathbb{E}_2\right)^\top$$

$$\tilde{\mathscr{G}}_{ij} = -Y\mathbb{E}_1 + YA_i\mathbb{E}_2 + YC_i\mathbb{E}_5 + YN_i\mathbb{E}_7 + YN_i\mathbb{E}_{8+\varrho_1} + U_j\mathbb{E}_{10+3\varrho_1}.$$

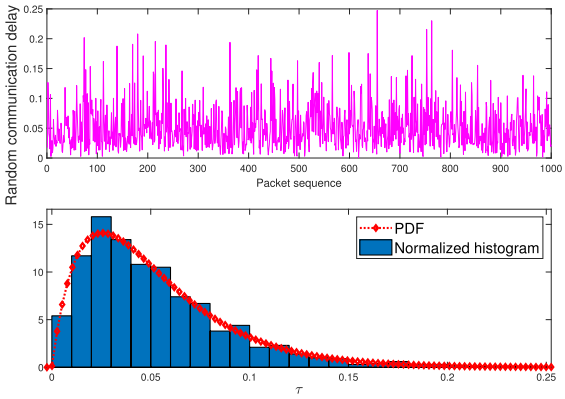

Fig. 1. Case I: Random communication delay and its pdf under $\tau_M = 0.25\ s$.

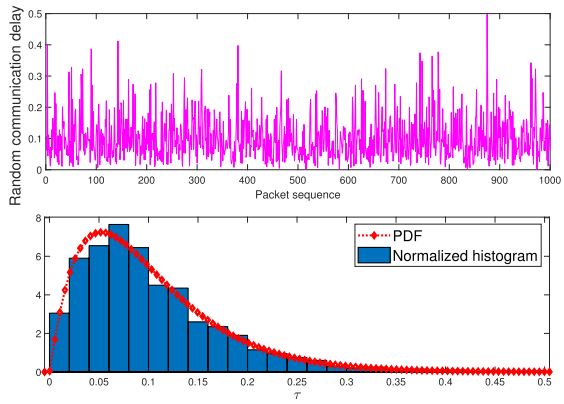

Fig. 2. Case II: Random communication delay and its pdf under $\tau_M = 0.5\ s$.

Then, the controller gain is derived as $K_j = Y^{-1}U_j$.

Proof: By introducing a new variable $U_j = YK_j$ and replacing YK_j in $\mathbf{He}(\mathscr{Y}\mathscr{G}_{ij})$ by U_j, it yields (23). Thus, the proof is fulfilled. ■

IV. Simulation Results

Example 1: For system (1), the following parameters are considered:

$$A_1=\begin{bmatrix}-2 & 0\\ 0 & -2\end{bmatrix}, N_1=\begin{bmatrix}-0.5 & 0.2\\ 0.2 & 0.5\end{bmatrix}, C_1=\begin{bmatrix}-2.3 & -0.2\\ 0.2 & -4.1\end{bmatrix}$$

$$A_2=\begin{bmatrix}-1 & 0\\ 0 & -1\end{bmatrix}, N_2=\begin{bmatrix}-1.5 & 0.2\\ 0.3 & -1\end{bmatrix}, C_2=\begin{bmatrix}-2.6 & -0.1\\ 0.4 & -3.8\end{bmatrix}$$

and $\psi(x_i) = tanh(\sigma_i) - tanh(\delta_i)$ satisfying (6) with $\Psi_1 = -I_2$ and $\Psi = I_2$.

The distributed delay kernel is selected as $g(s) = -10se^{5s}$, $s \in [-r(t), 0]$, $r(t) \in [r_1, r_2]$, $r_1 = 0.6$, and $r_2 = 0.8$. The derivative of $g(s)$ is obtained as $\dot{g}(s) = 5(-10ve^{5s}) + (-10e^{5s})$. According to (7), we choose $-10e^{5s}$ as another term in $\boldsymbol{g}(s)$, which gives

$$\boldsymbol{g}(s)=\begin{bmatrix}-10se^{5s}\\ -10e^{5s}\end{bmatrix}, \mathcal{G}=\begin{bmatrix}5 & 1\\ 0 & 5\end{bmatrix}, G(s)=\boldsymbol{g}(s)\otimes I_2, \widehat{\mathcal{G}}=\mathcal{G}\otimes I_2$$

$$\mho_1^{-1}=\int_{-r_1}^{0}\boldsymbol{g}(s)\boldsymbol{g}^{\top}(s)ds, \Omega_2^{-1}=\int_{-r_2}^{-r_1}\boldsymbol{g}(s)\boldsymbol{g}^{\top}(s)ds.$$

The probability distribution of the random communication delay is considered as Gamma distribution. The following two cases with different delay upper bound $\tau_M = 0.25s$ (Case I) and $\tau_M = 0.5s$ (Case II) are executed. The communication delay of the network and its normalized distribution histogram are drawn in Figs. 1 and 2, respectively.

In Case I with $\tau_M = 0.25s$, a probability density function $w(\tau)$ is used to approximate the distribution, and is chosen as

$$w(\tau) = 1600\tau e^{-40\tau}, \tau \in [0, \tau_M]$$

where $\int_0^{\tau_M} w(s)ds = 1$. In order to correspond to the form of $\int_{-\tau_M}^{0} w(s)x(t+s)ds$ in the derivations, $w(\tau)$ is written as $w(s) = w_0(s) = -1600se^{40s}$, $s \in [-\tau_M, 0]$. For $\varrho = 1$, to construct the vector $\boldsymbol{w}(s)$ satisfying (7), another term $w_1(s) = -40e^{40s}$ is chosen. Then, the vector $\boldsymbol{w}(s)$ and corresponding parameters are given as Case I

$$\boldsymbol{w}(s)=\begin{bmatrix}-1600\ se^{40s}\\ -1600e^{40s}\end{bmatrix}, \mathcal{W}=\begin{bmatrix}40 & 1\\ 0 & 40\end{bmatrix}.$$

In Case II $\tau_M = 0.5s$, $w(\tau)$ is chosen as

$$w(\tau) = 400\tau e^{-20\tau}, \tau \in [0, \tau_M]$$

where $\int_0^{\tau_M} w(s)ds = 1$. Following the similar way to construct the vector $\boldsymbol{w}(s)$ as:

$$\boldsymbol{w}(s)=\begin{bmatrix}-400se^{20s}\\ -400e^{20s}\end{bmatrix}, \mathcal{W}=\begin{bmatrix}20 & 1\\ 0 & 20\end{bmatrix}.$$

Taking the same manner for $g(s)$, one obtains

$$W(s) = \boldsymbol{w}(s)\otimes I_n, \widehat{\mathcal{W}} = \mathcal{W}\otimes I_n$$

$$\mho_3^{-1} = \int_{-\tau_M}^{0}\boldsymbol{w}(s)\boldsymbol{w}^{T}(s)ds.$$

We choose $\mu = 5$, $\nu = 20$, $\vartheta_1 = 0.1$, and $\vartheta_2 = 0.1$. By solving Theorem 2, the controller gains for two cases are given as follows.

Case I:

$$K_1=\begin{bmatrix}-12.0706 & 0.7972\\ 0.1501 & -12.1617\end{bmatrix},$$

$$K_2=\begin{bmatrix}-13.2206 & 0.9541\\ 0.1300 & -13.4511\end{bmatrix}.$$

Case II:

$$K_1=\begin{bmatrix}-7.3835 & 0.8028\\ 0.0294 & -6.9998\end{bmatrix}, K_2=\begin{bmatrix}-8.4202 & 0.8478\\ 0.0018 & -8.0860\end{bmatrix}.$$

In simulation, the initial conditions are chosen as $\delta(0) = [-0.5, 0.2]^{\top}$ and $\sigma(0) = [-1, 1]^{\top}$, and the simulation period is $0.01s$. The state responses of the primary and secondary systems without control are shown in Fig. 3. By using the designed controller, the curves of random delay, its probability

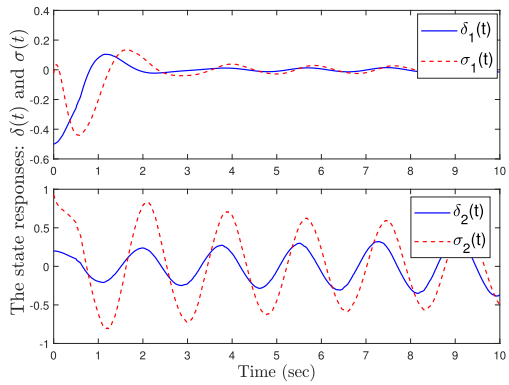

Fig. 3. State responses of the primary and secondary systems without control.

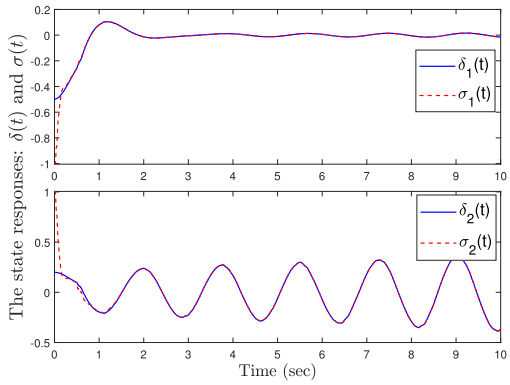

Fig. 4. Case I: State responses of the primary and secondary systems with control and $\tau_M = 0.25\ s$.

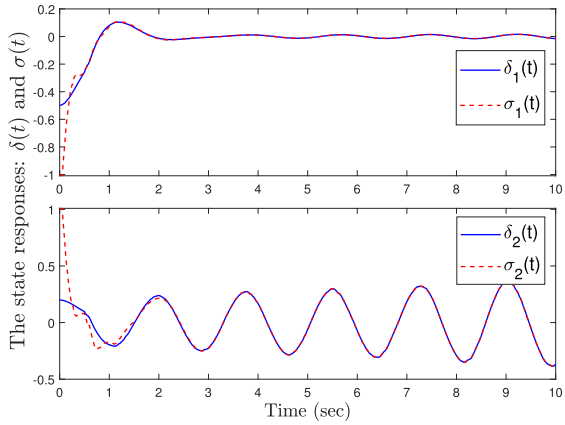

Fig. 5. State responses of the primary and secondary systems with control and $\tau_M = 0.5$ s.

density function (pdf), and the corresponding state responses for different τ_M are shown in Figs. 4 and 5. According to Fig. 3, one sees that the state trajectories of secondary system are not synchronized with the trajectories of primary system state without the utilization of control. In terms of Figs. 4 and 5, nevertheless, the primary system is well tracked by the secondary system through the developed controller (8). In addition, one also observes that the increase of network delay will decrease the synchronization performance.

Example 2: In this example, a practical system, the delayed memristor-based Chua's circuit with a flux-controlled memristor, is modeled as the considered system model (1). The dynamics of the memristor-based Chua's circuit is given by the following set of differential equations [37]:

$$\begin{cases} \dot{v}_1(t) = \left(-\frac{1}{\mathsf{RC}_1} - \frac{W(f(t))}{\mathsf{C}_1}\right) v_1(t) + \frac{1}{\mathsf{RC}_1} v_2(t) \\ \dot{v}_2(t) = \frac{1}{\mathsf{RC}_2} v_1(t) - \frac{1}{\mathsf{RC}_2} v_2(t) + \frac{1}{\mathsf{C}_2} i(t) \\ \dot{i}(t) = -\frac{1}{\mathsf{L}} v_2(t) - \frac{b_1}{\mathsf{L}} i(t) - \frac{b_2}{\mathsf{L}} \sin(v_1(t - r_1)) \\ \dot{\phi}(t) = v_1(t) \end{cases} \tag{24}$$

where

$$W(f(t)) = \dot{q}(f(t)) = \begin{cases} a_1, |f(t)| < 1; \\ a_2, |f(t)| > 1 \end{cases}$$

$$q(f(t)) = a_2 f(t) + 0.5(a_1 - a_2)(|f(t) + 1| - |f(t) - 1|).$$

With the same definitions of state variables and premise variable in [37], the state space model of memristor-based Chua's circuit with time delay can be represented by the proposed primary system (1) with $N_i = 0$ as

$$\dot{\delta}(t) = \sum_{i=1}^{2} \theta_i(t) \left[A_i \delta(t) + C_i \eta(\delta(t - r_1))\right] \tag{25}$$

where

$$\theta_1(t) = \begin{cases} 1, & |\delta_4(t)| \le 1 \\ 0, & |\delta_4(t)| > 1 \end{cases}, \theta_2(t) = \begin{cases} 0, & |\delta_4(t)| \le 1 \\ 1, & |\delta_4(t)| > 1 \end{cases}$$

$$A_1 = \begin{bmatrix} -\alpha_1 - \alpha_2 a_1 & \alpha_1 & 0 & 0 \\ \alpha_3 & -\alpha_3 & \alpha_4 & 0 \\ 0 & -\alpha_5 & -\alpha_6 & 0 \\ 1 & 0 & 0 & 0 \end{bmatrix}, C_1 = \begin{bmatrix} 0 & 0 & 0 & 0 \\ 0 & 0 & 0 & 0 \\ -\alpha_7 & 0 & 0 & 0 \\ 0 & 0 & 0 & 0 \end{bmatrix}$$

$$A_2 = \begin{bmatrix} -\alpha_1 - \alpha_2 a_2 & \alpha_1 & 0 & 0 \\ \alpha_3 & -\alpha_3 & \alpha_4 & 0 \\ 0 & -\alpha_5 & -\alpha_6 & 0 \\ 1 & 0 & 0 & 0 \end{bmatrix}, C_2 = C_1$$

$$\eta(\delta(t - r_1)) = \sin(\delta(t - r_1)), \frac{1}{\mathsf{RC}_1} = \alpha_1, \frac{1}{\mathsf{C}_1} = \alpha_2$$

$$\frac{1}{\mathsf{RC}_2} = \alpha_3, \frac{1}{\mathsf{C}_2} = \alpha_4, \frac{1}{\mathsf{L}} = \alpha_5, \frac{b_1}{\mathsf{L}} = \alpha_6, \frac{b_2}{\mathsf{L}} = \alpha_7.$$

Following the abovementioned way, another delayed memristor-based Chua's circuit viewed as the secondary system (3) with $N_i = 0$ can be derived, and the finial synchronization error system is established as

$$\dot{x}(t) = \sum_{i=1}^{2} \theta_i(t) \left[A_i x(t) + C_i \psi(x(t - r_1))\right] \tag{26}$$

where $\psi(x_i) = \sin(\sigma_i) - \sin(\delta_i)$ satisfying (6) with $\Psi_1 = -2I_2$ and $\Psi = 2I_2$.

In this example, the probabilistic communication delay with upper bound $\tau_M = 0.25s$ and the same distribution in Case I of Example 1 is considered. By choosing $\mu = 50$, $\nu = 20$, $\vartheta_1 = 0.1$, $\vartheta_2 = 0.1$, $r_1 = 0.1$, $\mathsf{C}_1 = 0.1$, $\mathsf{C}_2 = 1$, $\mathsf{L} = 1/18$,

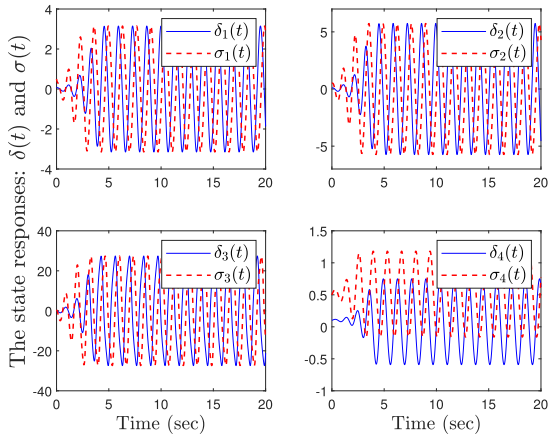

Fig. 6. State responses of the primary and secondary systems without control.

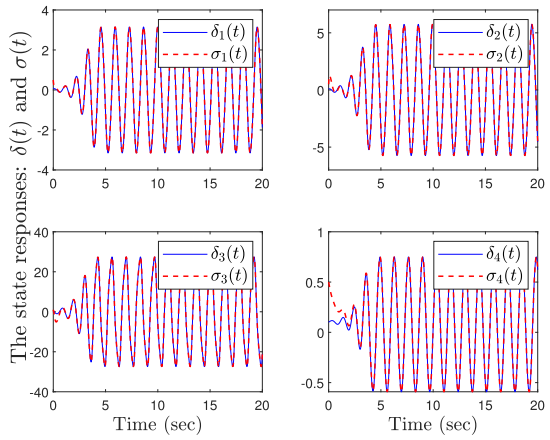

Fig. 7. State responses of the primary and secondary systems with control and $\tau_M = 0.25\ s$.

$b_1 = 1/45$, $\mathsf{R} = 1$, $a_1 = 0.3$, $a_2 = 0.8$, and $b_2 = 3$, and solving the conditions in Theorem 2, it gives

$$K_1 = \begin{bmatrix} -13.8486 & -6.5527 & -0.0720 & 0.0000 \\ 81.4348 & -8.0443 & 0.3376 & -0.0001 \\ 183.0534 & -37.5465 & -6.2931 & -0.0001 \\ -1.1116 & -0.2159 & -0.0062 & -1.0630 \end{bmatrix}$$

$$K_2 = \begin{bmatrix} -12.0849 & -6.2243 & -0.0635 & 0.0000 \\ 81.3364 & -8.0907 & 0.3360 & -0.0001 \\ 182.0873 & -37.7440 & -6.3123 & -0.0001 \\ -1.1117 & -0.2159 & -0.0062 & -1.0630 \end{bmatrix}.$$

In simulation, we set $\delta(0) = [0.1, 0.1, 0.1, 0.1]^\top$ and $\sigma(0) = [0.5, 0.5, 0.5, 0.5]^\top$, and the simulation period is $0.001s$. The state responses of the primary and secondary systems without control are shown in Fig. 6. Under the abovementioned designed fuzzy controller, the corresponding state responses are drawn in Fig. 7. In terms of these figures, it is seen that the primary and secondary systems are well synchronized by the proposed controller, while the primary system cannot be tracked by the secondary system without the effect of control input.

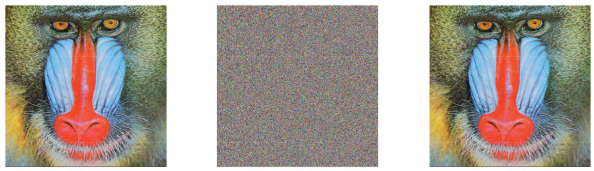

Fig. 8. (a) Original, (b) encrypted, and (c) decrypted images of Baboon under the encryption algorithm with $\wp = 2$. (a) Original image. (b) Encrypted image. (c) Decrypted image.

V. Simulation Results of Image Encryption

The system (1) synchronized via the controller solved by Theorem 2 is utilized to deal with the problem of image encryption. The same parameters for Case I in Example 1 are chosen to derive the controller, and the simulation is executed from 0to $800s$. For a color picture $\mathcal{F}$ of size $h \times l \times 3$, the following encryption algorithm is developed.

Step I: Convert the color image $\mathcal{F}(a, b, c)$, $a = 1, 2, \ldots, h$, $b = 1, 2, \ldots, l$, $c = 1, 2, 3$ into a matrix $\mathcal{O}(i, j)$, which is represented as

$$\mathcal{O}(i,j) = \begin{cases} \mathcal{F}(i, j, 1), & i = 1, \ldots, h \\ \mathcal{F}(i-h, j, 2), & i = h+1, \ldots, 2h \\ \mathcal{F}(i-2h, j, 3), & i = 2h+1, \ldots, 3h \end{cases} \tag{27}$$

where $j = 1, \ldots, l$.

Step II: When system (11) is stabilized at time t_1, three encryption keys with respect to the state $\delta(t)$ are given as

$$\mathcal{K}_1(i) = \circledcirc \big((10^5 \times |\delta_1(t_i) + \delta_2(t_i) - \odot(\delta_1(t_i) + \delta_2(t_i))|), 3h\big) + 1 \tag{28}$$

$$\mathcal{K}_2(j) = \circledcirc \big((10^5 \times |\delta_1(t_j) \times \delta_2(t_j) - \odot(\delta_1(t_j) \times \delta_2(t_j))|), n\big) + 1 \tag{29}$$

$$\mathcal{K}_3(v) = \circledcirc \big(10^5 \times |\delta_1(t_v) \times \delta_2(t_v) - \odot(\delta_1(t_v) - \delta_2(t_v))|), 256\big) \tag{30}$$

where $\circledcirc(a_1, a_2)$ returns the remainder after division of a_1 by a_2, $\odot(a)$ denotes the maximum integer less than or equal to a, $t_i \in \{t_1, t_2, \ldots, t_{3h}\}$, $t_j \in \{t_1, t_2, \ldots, t_l\}$, and $t_v \in \{t_1, t_2, \ldots, t_{3hl}\}$.

Step III: Take the $\mathcal{K}_1(i)$th row and the $\mathcal{K}_2(j)$th column as the ith row and jth column of $\mathcal{O}(i, j)$, and convert $\mathcal{O}(\mathcal{K}_1(i), \mathcal{K}_2(j))$ into a row vector $\mathcal{X}(k) \in \mathbb{R}^{1\times 3mn}$. Then, we define a new vector $\mathcal{X}$ as follows:

$$\mathcal{X}'(k) = \mathcal{X}(k) \oplus (\mathcal{X}(k) + \mathcal{K}_3(k)) \oplus \mathcal{X}'(k-1) \tag{31}$$

for $k = 1, \ldots, 3hl$, in which $\oplus$ denotes the logical operation. Then, $\mathcal{X}'$ is transformed into a $h \times l \times 3$ image $\mathcal{I}$.

Step IV: Repeat Steps I–III for $\wp$ times to obtain the cipher image $\hat{\mathcal{I}}$.

The decryption dependent on the state $\sigma(t)$ is the contrary process of encryption, which is not presented.

Then, a color picture named Baboon in Fig. 8 is applied to show the validity of the presented encryption algorithm. By

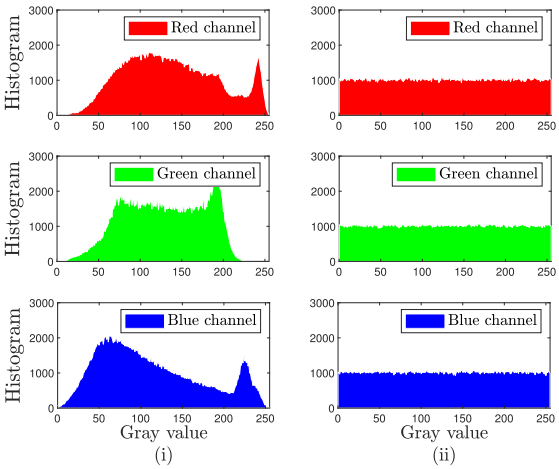

Fig. 9. Histograms of the (i) original Baboon and (ii) encrypted Baboon.

TABLE I
COMPARISON OF THE CORRELATION BETWEEN ADJACENT PIXELS

		Original picture	Encrypted picture
Red	H	0.9198	0.0175
	V	0.8545	-0.0044
	D	0.8425	0.0123
Green	H	0.8658	-0.0184
	V	0.7609	-0.0094
	D	0.7289	-0.0294
Blue	H	0.9021	0.0143
	V	0.8807	0.0030
	D	0.8330	-0.0195

setting $\wp = 2$ and executing the encryption algorithm for the image Baboon, the histograms of the three colors of Fig. 6 are shown in Fig. 9. From Fig. 8, one can observe that a clear and complete decrypted image can be derived by our encryption algorithm, when the primary–secondary systems are synchronized. Furthermore, Fig. 9 shows that the encrypted picture histograms nearly satisfy uniform distribution, which means a more random tonal distribution of the picture can be obtained.

The correlation between contiguous pixels is given as follows:

$$\jmath_{xy} = \ell(x,y)/(\sqrt{\imath(x)}\sqrt{\imath(y)}) \tag{32}$$

where

$$\ell(x,y) = \frac{1}{\aleph}\sum_{i=1}^{\aleph}(x_i - \Im(x))(y_i - \Im(y))$$

$$\imath(x) = \frac{1}{\aleph}\sum_{i=1}^{\aleph}(x_i - \Im(x))^2, \Im(x) = \frac{1}{\aleph}\sum_{i=1}^{\aleph}x_i$$

where x and y are two adjacent pixel values in the plain image or the cipher image, $\aleph$ is the number of pixels testing, and $\Im(\cdot)$ means the mathematical expectation. The correlation between two adjacent pixels in horizontal, vertical, and diagonal directions computed by (32) is tabulated in Table I. Fig. 10 shows the scatter diagram of the correlation. The results in Table I demonstrate that the correlation of the encrypted picture is around 0, which is much smaller than the value close to 1 of the original one. Meanwhile, Fig. 10 shows that the scatter diagram

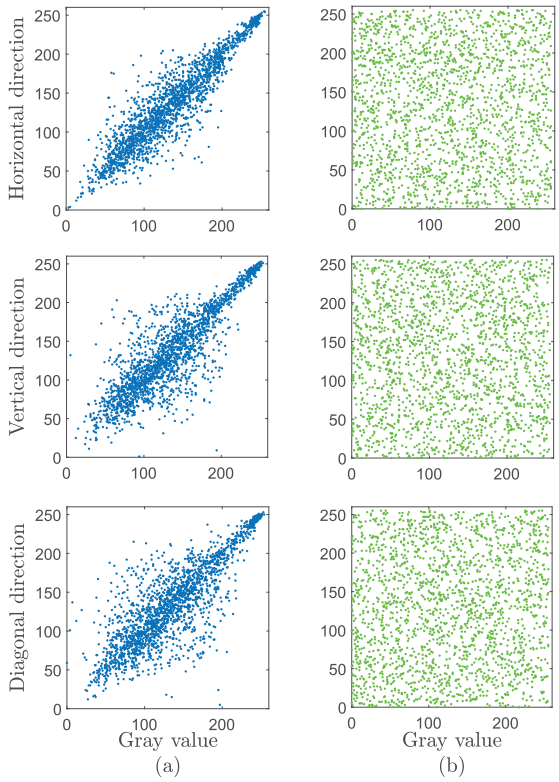

Fig. 10. Red channel: the scatter diagram for correlation of (a) original Baboon and (b) encrypted Baboon in horizontal, vertical, and diagonal directions.

TABLE II
INFORMATION ENTROPY OF THE ORIGINAL AND THE ENCRYPTED PICTURES

	Encrypted picture	Original picture
Red	7.9914	7.7064
Green	7.9916	7.4744
Blue	7.9917	7.5722

of the cipher image is more random than the scatter diagram of the original image.

In addition, the information entropy reflecting the uncertain degree of the encrypted image is tabulated in Table II. According to the theory of information, if the information entropy value equal to 8, it means the highest uncertain degree of a picture. The results in Table II tell that the encrypted picture is much more uncertain than the original one.

The abovementioned analysis implies that the developed algorithm is effective to make the encrypted image more stochastic and uncertain, which is helpful for improving the reliability of encryption process.

VI. CONCLUSION

This article has handled the synchronization of fuzzy NNs with time-varying distributed delay and stochastic network delay. A united distributed delay system was formed to describe the fuzzy NNs with time-varying distributed delay and stochastic network delay. In terms of the constructed LKF and the integral inequality, some novel criteria were presented to ensure the synchronization error system to be stable. The effectiveness of

the addressed method was illustrated by the simulation results of the numerical example and the image encryption issue. It is known that the resource of real communication network is usually limited and the event-triggered scheme is an effective way to save network resource. In the future, therefore, the combination of the developed delay modeling method and event-triggered scheme for networked systems will be investigated.

APPENDIX

Proof of Theorem 1

For the selected LKF (17), by using Lemma 1, it leads to

$$\int_{-r_1}^{0} \mathbf{Sy}\left(S_1, \psi(x(t+s))\right) ds \geq \mathbf{Sy}\left(\mathcal{S}_1, \mathbb{G}_1(t)\right). \tag{33}$$

Applying Lemma 2 to relax the integral term $\int_{-r_2}^{-r_1} \mathbf{Sy}(S_2, \psi(x(t+s)))ds$ in LKF (17) yields

$$\begin{aligned}&\int_{-r_2}^{-r_1} \mathbf{Sy}\left(S_2, \psi(x(t+s))\right) ds \\ &\quad\geq \mathbf{Sy}\left(\mathcal{S}_2, \begin{bmatrix} \mathbb{C}_{n,\varrho_1+1} & 0_{n(\varrho_1+1)} \\ 0_{n(\varrho_1+1)} & \mathbb{C}_{n,\varrho_1+1} \end{bmatrix} \begin{bmatrix} \mathbb{G}_3(t) \\ \mathbb{G}_4(t) \end{bmatrix}\right).\end{aligned} \tag{34}$$

By taking the similar way to obtain (33), the following inequality:

$$\int_{-\tau_M}^{0} \mathbf{Sy}\left(S_3, x(t+s)\right) ds \geq \mathbf{Sy}\left(\mathcal{S}_3, \mathbb{W}(t)\right) \tag{35}$$

can be derived by replacing the kernel $G(s)$ and function $\boldsymbol{g}(s)$ in Lemma 1 with $W(s)$ and $\boldsymbol{w}(s)$, respectively.

Therefore, from (17), (33), and (34), one has

$$\begin{aligned}V(t) \geq\ & \mathbf{Sy}\left(\mathcal{P}, \varkappa(t)\right) + \int_{-\tau_M}^{0} \mathbf{Sy}\left(R_3, x(t+s)\right) ds \\ &+ \int_{-r_1}^{0} \mathbf{Sy}\left((s+r_1)R_1, \psi(x(t+s)\right) ds \\ &+ \int_{-r_2}^{-r_1} \mathbf{Sy}\left((s+r_2)R_2, \psi(x(t+s)\right) ds.\end{aligned} \tag{36}$$

From $S_1 > 0, R_1 > 0, S_2 > 0, R_2 > 0, S_3 > 0, R_3 > 0$, and $\mathcal{P} > 0, V(t) > 0$ is satisfied.

In terms of the property (7), it gives

$$\dot{\mathbb{G}}_1(t) = G(0)\psi(x(t)) - G(-r_1)\psi(x(t-r_1)) - \widehat{\mathcal{G}}\mathbb{G}_1(t) \tag{37}$$

$$\begin{aligned}\dot{\mathbb{G}}_2(t) =\ & G(-r_1)\psi(x(t-r_1)) \\ &- G(-r_2)\psi(x(t-r_2)) - \widehat{\mathcal{G}}\mathbb{G}_2(t)\end{aligned} \tag{38}$$

$$\dot{\mathbb{W}}(t) = W(0)x(t) - W(-\tau_M)x(t-\tau_M) - \widehat{\mathcal{W}}\mathbb{W}(t) \tag{39}$$

where $\widehat{\mathcal{G}} = \mathcal{G} \otimes I_{(\varrho_1+1)n}$ and $\widehat{\mathcal{W}} = \mathcal{W} \otimes I_{(\varrho_2+1)n}$.

Then, the system stability is ensured by $\dot{V}(t) < 0$, where

$$\begin{aligned}\dot{V}(t) \leq\ & 2\varkappa^T(t)P\dot{\varkappa}(t) + \mathbf{Sy}\left(S_1 + r_1R_1, \psi(x(t))\right) \\ &+ \mathbf{Sy}\left(S_2 + r_3R_2 - S_1, \psi(x(t-r_1))\right) \\ &- \mathbf{Sy}\left(S_2, \psi(x(t-r_2))\right) + \mathbf{Sy}\left(S_3 + \tau_M R_3, x(t)\right) \\ &- \mathbf{Sy}\left(S_3, x(t-\tau_M)\right) - \int_{-r_1}^{0} \mathbf{Sy}\left(R_1, \psi(x(t+s))\right) ds \\ &- \int_{-r_2}^{-r_1} \mathbf{Sy}(R_2, \psi(x(t+s))\, ds - \int_{-\tau_M}^{0} \mathbf{Sy}(R_3, x(t+s))\, ds.\end{aligned} \tag{40}$$

With the help of [35, Lem. 5], it yields

$$-\int_{-r_1}^{0} \mathbf{Sy}\left(R_1, \psi(x(t+s))\right) ds \leq -\mathbf{Sy}\left(\mathcal{R}_1, \mathbb{G}_1(t)\right) \tag{41}$$

$$-\int_{-\tau_M}^{0} \mathbf{Sy}\left(R_3, x(t+s)\right) ds \leq -\mathbf{Sy}\left(\mathcal{R}_3, \mathbb{W}(t)\right). \tag{42}$$

According to Lemma 2, we have

$$\begin{aligned}&-\int_{-r_2}^{-r_1} \mathbf{Sy}\left(R_2, \psi(x(t+s))\right) ds \\ &\quad\leq -\mathbf{Sy}\left(\mathcal{R}_2, \begin{bmatrix} \mathbb{C}_{n,\varrho_1+1} & 0_{n(\varrho_1+1)} \\ 0_{n(\varrho_1+1)} & \mathbb{C}_{n,\varrho_1+1} \end{bmatrix} \begin{bmatrix} \mathbb{G}_3(t) \\ \mathbb{G}_4(t) \end{bmatrix}\right).\end{aligned} \tag{43}$$

By defining $\zeta^\top(t) = [\dot{x}^\top(t), x^\top(t), x^\top(t-\tau_M), \psi^\top(x(t)), \psi^\top(x(t-r_1)), \psi^\top(x(t-r_2)), \mathbb{G}_1^\top(t), \mathbb{G}_3^\top(t), \mathbb{G}_4^\top(t), \mathbb{W}^\top(t)]$, the system (14) can be expressed as

$$\sum_{i=1}^{p}\sum_{j=1}^{p} \theta_i\theta_j^\tau \mathscr{G}_{ij}\zeta(t) = 0. \tag{44}$$

In terms of the description of system (14), it gives

$$\varkappa(t) = \mathbb{M}\zeta(t), \dot{\varkappa}(t) = \mathbb{H}\zeta(t). \tag{45}$$

Based on (6), one can get

$$\mathbf{Sy}\left(\begin{bmatrix} \Phi_1 & \Phi_2 \\ & I \end{bmatrix}, \begin{bmatrix} x(t) \\ \psi(x(t)) \end{bmatrix}\right) < 0 \tag{46}$$

which results in

$$-\nu\mathbf{Sy}\left(\Phi, \mathcal{E}_1\zeta(t)\right) > 0. \tag{47}$$

To guarantee the stability of system (14), one needs

$$\dot{V}(t) \leq \sum_{i=1}^{p}\sum_{j=1}^{p} \theta_i\theta_j^\tau \zeta^\top(t)\Gamma_{ij}\zeta(t) < 0. \tag{48}$$

For the defined $\mathscr{Y}$ and (44), it leads to

$$\sum_{i=1}^{p}\sum_{j=1}^{p} \theta_i\theta_j^\tau \mathscr{Y}\mathscr{G}_{ij}\zeta(t) = 0. \tag{49}$$

From (47)–(49), it gives

$$\sum_{i=1}^{p}\sum_{j=1}^{p} \theta_i\theta_j^\tau \zeta^\top(t)\Pi_{ij}\zeta(t) < 0 \tag{50}$$

where $\Pi_{ij} = \Gamma_{ij} + \mathbf{He}(\mathscr{Y}\mathscr{G}_{ij}) - \nu\mathbf{Sy}(\mathcal{L}, \mathcal{E}_1)$.

Choose a free matrix $\digamma = \digamma^T < 0$ such that

$$\sum_{i=1}^{p}\sum_{j=1}^{p} \theta_i(\theta_j - \theta_j^\tau)\zeta^\top(t)\digamma\zeta(t) = 0. \tag{51}$$

Combing (50) and (51), we have

$$\begin{aligned}
&\sum_{i=1}^{p}\sum_{j=1}^{p}\theta_i\theta_j^{\tau}\zeta^{\top}(t)\Pi_{ij}\zeta(t)\\
&\le \sum_{i=1}^{p}\sum_{j=1}^{p}\theta_i\theta_j^{\tau}\zeta^{\top}(t)\Pi_{ij}\zeta(t)-\varpi^{\top}(t)\digamma\varpi(t)\\
&=\zeta^{\top}(t)\left[\sum_{i=1}^{p}\sum_{j=1}^{p}\theta_i\theta_j^{\tau}(\Pi_{ij}-(\digamma_{i,j+p}+\digamma_{j+p,i}))\right.\\
&\quad-\sum_{i=1}^{p}\sum_{j=1}^{p}\theta_i\theta_j\frac{(\digamma_{i,j}+\digamma_{j,i})}{2}\\
&\quad\left.-\sum_{i=1}^{p}\sum_{j=1}^{p}\theta_i^{\tau}\theta_j^{\tau}\frac{(\digamma_{i+p,j+p}+\digamma_{j+p,i+p})}{2}\right]\zeta(t) \qquad (52)
\end{aligned}$$

where $\varpi(t)=\left[\theta_1 I\zeta(t)\cdots\theta_p I\zeta(t)\theta_1^{\tau}I\zeta(t)\cdots\theta_p^{\tau}I\zeta(t)\right]$.

Then, from the fact that $\sum_{i=1}^{p}\sum_{j=1}^{p}\theta_i(\theta_j-\theta_j^{\tau})\beth_{1i}=0$ and $\sum_{i=1}^{p}\sum_{j=1}^{p}(\theta_i-\theta_i^{\tau})\theta_j^{\tau}\beth_{2j}=0$, by utilizing [36, Lem. 1] to deal with the asynchronous premises θ_j^{τ} and θ_j, one has

$$\begin{aligned}
&\sum_{i=1}^{p}\sum_{j=1}^{p}\theta_i\theta_j^{\tau}\zeta^{\top}(t)\Pi_{ij}\zeta(t)-\varpi^{\top}(t)\digamma\varpi(t)\\
&=\zeta^{\top}(t)\left[\sum_{i=1}^{p}\sum_{j=1}^{p}\theta_i\theta_j^{\tau}\left(\Pi_{ij}-(\digamma_{i,j+p}+\digamma_{j+p,i})\right.\right.\\
&\quad\left.-\frac{(\digamma_{i,j}+\digamma_{j,i})}{2}-\frac{(\digamma_{i+p,j+p}+\digamma_{j+p,i+p})}{2}\right)\\
&\quad+\sum_{i=1}^{p}\sum_{j=1}^{p}\theta_i(\theta_j-\theta_j^{\tau})\left(\beth_{1i}-\frac{(\digamma_{i,j}+\digamma_{j,i})}{2}\right)\\
&\quad\left.+\sum_{i=1}^{p}\sum_{j=1}^{p}(\theta_i^{\tau}-\theta_i)\theta_j^{\tau}\left(\beth_{2j}-\frac{(\digamma_{i+p,j+p}+\digamma_{j+p,i+p})}{2}\right)\right]\zeta(t)\\
&\le\zeta^{\top}(t)\sum_{i=1}^{p}\sum_{j=1}^{p}\theta_i\theta_j^{\tau}(\Pi_{ij}+\Theta_{ij})\zeta(t) \qquad (53)
\end{aligned}$$

where $\beth_{1i}-\frac{(\digamma_{i,l}+\digamma_{l,i})}{2}>0$ and $\beth_{2j}-\frac{(\digamma_{l+p,j+p}+\digamma_{j+p,l+p})}{2}>0$ are ensured by (21) and (22), respectively. Thus, the proof is completed. ■

REFERENCES

[1] S. Delprat, J. Alvarez, M. Sanchez, and M. Bernal, "A tighter exact convex modelling for improved LMI-based nonlinear system analysis and design," *IEEE Trans. Fuzzy Syst.*, vol. 29, no. 9, pp. 2819–2824, Sep. 2021.

[2] Z. Feng, Y. Yang, and H. K. Lam, "Extended-dissipativity-based adaptive event-triggered control for stochastic polynomial fuzzy singular systems," *IEEE Trans. Fuzzy Syst.*, Aug. 2021, early access, Aug. 25, 2021, doi: 10.1109/TFUZZ.2021.3107753.

[3] N. Gunasekaran, G. Zhai, and Q. Yu, "Exponential sampled–data fuzzy stabilization of nonlinear systems and its application to basic buck converters," *IET Control Theory Appl.*, vol. 15, pp. 9, pp. 1157–1168, Mar. 2021.

[4] S. Yan, Z. Gu, J. H. Park, and X. Xie, "Adaptive memory-event-triggered static output control of TS fuzzy wind turbine systems," *IEEE Trans. Fuzzy Syst.*, Dec. 2021, early access, Dec. 9, 2021, doi: 10.1109/TFUZZ.2021.3133892.

[5] B. Thangavel, S. Srinivasan, T. Kathamuthu, G. Zhai, and N. Gunasekaran, "Dynamical analysis of T–S fuzzy financial systems: A sampled-data control approach," *Int. J. Fuzzy Syst.*, vol. 24, pp. 1944–1957, 2022, doi: 10.1007/s40815-022-01249-4.

[6] X. Chang and G. Yang, "Nonfragile H_∞ filtering of continuous-time fuzzy systems," *IEEE Trans. Signal Process*, vol. 59, no. 4, pp. 1528–1538, Apr. 2011.

[7] X. Chang, "H_∞ filter design for T–S fuzzy systems with D stability constraints," *Control Decis.*, vol. 26, no. 7, pp. 1051–1055, Jul. 2011.

[8] N. Gunasekaran and Y. H. Joo, "Robust sampled-data fuzzy control for nonlinear systems and its applications: Free-weight matrix method," *IEEE Trans. Fuzzy Syst.*, vol. 27, no. 11, pp. 2130–2139, Nov. 2019.

[9] S. Yan, M. Shen, S. K. Nguang, G. Zhang, and L. Zhang, "A distributed delay method for event-triggered control of T–S fuzzy networked systems with transmission delay," *IEEE Trans. Fuzzy Syst.*, vol. 27, no. 10, pp. 1963–1973, Oct. 2019.

[10] H. Shen, T. Wang, J. Cao, G. Lu, Y. Song, and T. Huang, "Nonfragile dissipative synchronization for Markovian memristive neural networks: A gain-scheduled control scheme," *IEEE Trans. Neural Netw. Learn. Syst.*, vol. 30, no. 6, pp. 1841–1853, Jun. 2018.

[11] S. Lakshmanan, M. Prakash, C. P. Lim, R. Rakkiyappan, P. Balasubramaniam, and S. Nahavandi, "Synchronization of an inertial neural network with time-varying delays and its application to secure communication," *IEEE Trans. Neural Netw. Learn. Syst.*, vol. 29, no. 1, pp. 195–207, Jan. 2018.

[12] N. Gunasekaran, N. M. Thoiyab, Q. Zhu, J. Cao, and P. Muruganantham, "New global asymptotic robust stability of dynamical delayed neural networks via intervalized interconnection matrices," *IEEE Trans. Cybern.*, Jun. 2021, early access, Jun. 7, 2021, doi: 10.1109/TCYB.2021.3079423.

[13] S. Ding, Z. Wang, and X. Xie, "Periodic event-triggered synchronization for discrete-time complex dynamical networks," *IEEE Trans. Neural Netw. Learn. Syst.*, Feb. 2021, early access, Feb. 5, 2021, doi: 10.1109/TNNLS.2021.3053652.

[14] Z. Fei, C. Guan, and H. Gao, "Exponential synchronization of networked chaotic delayed neural network by a hybrid event trigger scheme," *IEEE Trans. Neural Netw. Learn. Syst.*, vol. 29, no. 6, pp. 2558–2567, 2017.

[15] S. Yan, S. K. Nguang, and Z. Gu, "H_∞ weighted integral event-triggered synchronization of neural networks with mixed delays," *IEEE Trans. Ind. Inform.*, vol. 17, no. 4, pp. 2365–2375, Apr. 2021.

[16] J. Xiao, J. Cheng, K. Shi, and R. Zhang, "A general approach to fixed-time synchronization problem for fractional-order multi-dimension-valued fuzzy neural networks based on memristor," *IEEE Trans. Fuzzy Syst.*, vol. 30, no. 4, pp. 968–977, Apr. 2022, doi: 10.1109/TFUZZ.2021.3051308.

[17] J. Wang, X. Wang, N. Xie, J. Xia, and H. Shen, "Fuzzy-model-based H_∞ pinning synchronization for coupled neural networks subject to reaction-diffusion," *IEEE Trans. Fuzzy Syst.*, vol. 30, no. 1, pp. 248–257, Jan. 2022.

[18] A. Mohammadzadeh, S. Ghaemi, O. Kaynak, and S. Khanmohammadi, "Robust H_∞-based synchronization of the fractional-order chaotic systems by using new self-evolving nonsingleton type-2 fuzzy neural networks," *IEEE Trans. Fuzzy Syst.*, vol. 24, no. 6, pp. 1544–1554, Dec. 2016.

[19] C. Huang, X. Zhang, H. K. Lam, and S. H. Tsai, "Synchronization analysis for nonlinear complex networks with reaction-diffusion terms using fuzzy-model-based approach," *IEEE Trans. Fuzzy Syst.*, vol. 29, no. 6, pp. 1350–1362, Jun. 2021.

[20] E. Yucel, M. S. Ali, N. Gunasekaran, and S. Arik, "Sampled-data filtering of Takagi–Sugeno fuzzy neural networks with interval time-varying delays," *Fuzzy Sets Syst.*, vol. 316, pp. 69–81, Jun. 2017.

[21] L. Song, S. K. Nguang, and D. Huang, "Hierarchical stability conditions for a class of generalized neural networks with multiple discrete and distributed delays," *IEEE Trans. Neural Netw. Learn. Syst.*, vol. 30, no. 2, pp. 636–642, Feb. 2018.

[22] A. Seuret, F. Gouaisbaut, and Y. Ariba, "Complete quadratic Lyapunov functionals for distributed delay systems," *Automatica*, vol. 62, pp. 168–176, Dec. 2015.

[23] D. Wu, M. Chen, and H. Gong, "Adaptive neural flight control for an aircraft with time-varying distributed delays," *Neurocomputing*, vol. 307, pp. 130–145, Sep. 2016.

[24] L. Zhang, H. Gao, and O. Kaynak, "Network-induced constraints in networked control systems—A survey," *IEEE Trans. Ind. Inform.*, vol. 9, no. 1, pp. 403–416, Feb. 2012.

[25] Y. Wang, Q. Han, M. Fei, and C. Peng, "Network-based T–S fuzzy dynamic positioning controller design for unmanned marine vehicles," *IEEE Trans. Cybern.*, vol. 48, no. 9, pp. 2750–2763, Sep. 2018.

[26] S. Yan, M. Shen, S. K. Nguang, and G. Zhang, "Event-triggered H_∞ control of networked control systems with distributed transmission delay," *IEEE Trans. Autom. Control*, vol. 65, no. 10, pp. 4295–4301, Oct. 2020.
[27] P. Park, J. W. Ko, and C. Jeong, "Reciprocally convex approach to stability of systems with time-varying delays," *Automatica*, vol. 47, no. 1, pp. 235–238, Jan. 2011.
[28] D. Yue, E. Tian, and Q.-L. Han, "A delay system method for designing event-triggered controllers of networked control systems," *IEEE Trans. Autom. Control*, vol. 58, no. 2, pp. 475–481, Feb. 2013.
[29] E. Tian and C. Peng, "Memory-based event-triggering H_∞ load frequency control for power systems under deception attacks," *IEEE Trans. Cybern.*, vol. 50, no. 11, pp. 4610–4618, Nov. 2020.
[30] F. Lian, J. Moyne, and D. Tilbury, "Network design consideration for distributed control systems," *IEEE Trans. Control Syst. Technol.*, vol. 10, no. 2, pp. 297–307, Mar. 2002.
[31] H. Yan, H. Zhang, F. Yang, X. Zhan, and C. Peng, "Event-triggered asynchronous guaranteed cost control for Markov jump discrete-time neural networks with distributed delay and channel fading," *IEEE Trans. Neural Netw. Learn. Syst.*, vol. 29, no. 8, pp. 3588–3598, Aug. 2018.
[32] H. Bao, J. H. Park, and J. Cao, "Exponential synchronization of coupled stochastic memristor-based neural networks with time-varying probabilistic delay coupling and impulsive delay," *IEEE Trans. Neural Netw. Learn. Syst.*, vol. 27, no. 1, pp. 190–201, Jan. 2016.
[33] Q. Feng, S. K. Nguang, and W. Perruquetti, "Dissipative stabilization of linear systems with time-varying general distributed delays," *Automatica*, vol. 122, Dec. 2020, Art. no. 109227.
[34] N. J. Higham, "The matrix computation toolbox for MATLAB (version 1.0)," 2002.
[35] Q. Feng and S. K. Nguang, "Stabilization of uncertain linear distributed delay systems with dissipativity constraints," *Syst. Control Lett.*, vol. 96, pp. 60–71, Oct. 2016.
[36] D. Zhang, Q. L. Han, and X. Jia, "Network-based output tracking control for T–S fuzzy systems using an event-triggered communication scheme," *Fuzzy Sets Syst.*, vol. 273, pp. 26–48, Aug. 2015.
[37] T. Lin, F. Huang, Z. Du, and Y. Lin, "Synchronization of fuzzy modeling chaotic time delay memristor-based Chua's circuits with application to secure communication," *Int. J. Fuzzy Syst.*, vol. 17, no. 2, pp. 206–214, Mar. 2015.

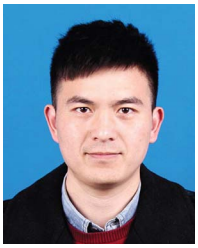

Shen Yan received the B.E. degree in automation and the Ph.D. degree in power engineering automation from the College of Electrical Engineering and Control Science of Nanjing Technology University, Nanjing, China, in 2014 and 2019, respectively.

From 2017 to 2018, he was a Visiting Ph.D. Student with the University of Auckland, Auckland, New Zealand. From February 2022 to August 2022, he was a Visiting Scholar with Yeungnam University, Gyeongsan, South Korea. He is currently an Associate Professor with the College of Mechanical and Electronic Engineering, Nanjing Forestry University, Nanjing. His current research interests include networked control systems, event-triggered control, and their applications.

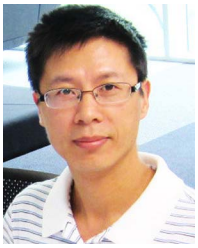

Zhou Gu (Member, IEEE) received the B.S. degree in automation from North China Electric Power University, Beijing, China, in 1997, and the M.S. and the Ph.D. degrees in control science and engineering from the Nanjing University of Aeronautics and Astronautics, Nanjing, China, in 2007 and 2010, respectively.

From 1996 to 2013, he was an Associate Professor with the School of Power Engineering, Nanjing Normal University, Nanjing. He was a Visiting Scholar with Central Queensland University, Rockhampton, QLD, Australia, and the University of Manchester, Manchester, U.K. He is currently a Professor with Nanjing Forestry University, Nanjing, China. His current research interests include networked control systems, time-delay systems, reliable control, and their applications.

Ju H. Park (Senior Member, IEEE) received the Ph.D. degree in electronics and electrical engineering from the Pohang University of Science and Technology (POSTECH), Pohang, South Korea, in 1997.

From May 1997 to February 2000, he was a Research Associate with Engineering Research Center-Automation Research Center, POSTECH. In March 2000, he joined Yeungnam University, Kyongsan, South Korea, where he is currently the Chuma Chair Professor. He is a co-author of the monographs *Recent Advances in Control and Filtering of Dynamic Systems with Constrained Signals* (Springer-Nature, 2018) and *Dynamic Systems With Time Delays: Stability and Control* (Springer-Nature, 2019), and edited a volume *Recent Advances in Control Problems of Dynamical Systems and Networks* (Springer-Nature, 2020). He has authored or coauthored a number of articles in the areas of his research interests, which include robust control and filtering, neural/complex networks, fuzzy systems, multiagent systems, and chaotic systems.

Dr. Park is a Fellow of the Korean Academy of Science and Technology (KAST). Since 2015, he has been the recipient of the Highly Cited Researchers Award by Clarivate Analytics (formerly, Thomson Reuters) and listed in three fields, Engineering, Computer Sciences, and Mathematics, in 2019–2021. He is currently the Editor of the *International Journal of Control, Automation and Systems*, and Subject Editor/Advisory Editor/Associate Editor/Editorial Board Member of several international journals, including *IET Control Theory & Applications, Applied Mathematics and Computation, Journal of The Franklin Institute, Nonlinear Dynamics, Engineering Reports, Cogent Engineering*, IEEE TRANSACTION ON FUZZY SYSTEMS, IEEE TRANSACTION ON NEURAL NETWORKS AND LEARNING SYSTEMS, and IEEE TRANSACTION ON CYBERNETICS.

Xiangpeng Xie (Member, IEEE) received the B.S. and Ph.D. degrees in engineering from Northeastern University, Shenyang, China, in 2004 and 2010, respectively.

From 2010 to 2014, he was a Senior Engineer with the Metallurgical Corporation of China Ltd., Beijing, China. He is currently a Professor with the Institute of Advanced Technology, Nanjing University of Posts and Telecommunications, Nanjing, China. His research interests include fuzzy modeling and control synthesis, state estimations, optimization in process industries, and intelligent optimization algorithms.

Dr. Xie is an Associate Editor for the *International Journal of Control, Automation, and Systems*, and the *International Journal of Fuzzy Systems*.